Novel pathways in cholesterol metabolism to combat cardiometabolic diseases

Zhou, E.

3

Hepatic SRB1 knockdown reduces atherosclerosis and enhances the anti-atherosclerotic effect of brown fat activation in APOE*3-Leiden.CETP mice

Enchen Zhou, Zhuang Li, Hiroyuki Nakashima, Cong Liu, Zhixiong Ying, Amanda C. Foks, Jimmy F.P. Berbée, Ko Willems van Dijk, Patrick C.N. Rensen, Yanan Wang

Arterioscler Thromb Vasc Biol 2021; Apr;41(4):1474-1486

Abstract

Background

Brown fat activation attenuates atherosclerosis development by accelerating triglyceride-rich lipoprotein turnover and/or stimulation of reverse cholesterol transport via the scavenger receptor class B type 1 (SRB1). The aim of this study was to investigate the specific role of hepatic SRB1 in the atheroprotective properties of brown fat activation.

Methods and results

*APOE*3-Leiden.CETP* mice, a well-established model of human-like lipoprotein metabolism and atherosclerosis, were treated with vehicle or AAV8-shRNA which decreased hepatic SRB1 protein levels by 40-55%. After 2 weeks, mice without or with hepatic SRB1 knockdown were treated with vehicle or the β3-adrenergic receptor (AR) agonist CL316,243 to activate brown fat for 4 weeks to determine HDL catabolism and for 9 weeks to evaluate atherosclerosis. Surprisingly, hepatic SRB1 knockdown additively improved the beneficial effects of β3-AR agonism on atherosclerosis development. In fact, hepatic SRB1 knockdown *per se* not only increased HDL-cholesterol levels, but also reduced plasma triglyceride and non-HDL-cholesterol levels, thus explaining the reduction in atherosclerosis development. Mechanistic studies indicated that this is due to increased lipolytic processing and hepatic uptake of VLDL by facilitating VLDL-surface transfer to HDL.

Conclusions

Hepatic SRB1 knockdown in a mouse model with an intact ApoE-LDLR clearance pathway, relevant to human lipoprotein metabolism, reduced atherosclerosis and improved the beneficial effect of brown fat activation on atherosclerosis development, explained by pleiotropic effects of hepatic SRB1 knockdown on lipolytic processing and hepatic uptake of VLDL. Brown fat activation could thus be an effective strategy to treat cardiovascular disease also in subjects with impaired SRB1 function.

Introduction

Atherosclerosis remains the most common cause of cardiovascular diseases. A prominent risk factor for atherosclerosis is dyslipidaemia, i.e. high levels of plasma low density lipoprotein-cholesterol (LDL-C) and triglycerides (TG), and low levels of high density lipoprotein-cholesterol (HDL-C). Remarkable efforts have been put into developing lipid-lowering medications such as statins and PCSK9 inhibitors. However, only 30% of all cardiovascular events can be prevented by such treatment strategies [1-3], illustrating the need for new therapeutic strategies.

Brown fat is an emerging target to combat cardiometabolic diseases [4-6]. We previously showed that brown fat activation by cold exposure and β3-AR agonism induces lipoprotein lipase (LPL)-mediated lipolysis of triglyceride-rich lipoproteins (TRLs), thereby reducing plasma triglycerides. The generated cholesterol-enriched TRL remnants are subsequently taken up by the liver thus reducing circulating (V)LDL-C levels and ameliorating atherosclerosis in *APOE*3-Leiden.CETP* (*E3L.CETP*) mice [7]. Nevertheless, the cholesterol-lowering effects explained only approx. 30% of atheroprotective effects of brown fat activation.

Interestingly, β3-AR agonism also increases HDL-C in both *E3L.CETP* mice [8] and in humans [9]. A human study further shows that brown fat activation by short-term cooling increases small HDL particles with increased cholesterol efflux capacity *in vitro* [10]. The increase in HDL may well contribute to the anti-atherogenic effect of brown fat activation, especially since β3-AR agonism promotes reverse cholesterol transport (RCT) as dependent on the hepatic scavenger receptor class B type 1 (SRB1) in mice [8].

SRB1 is highly expressed by hepatocytes and facilitates the selective uptake of HDL-derived cholesteryl esters [11]. SRB1-deficiency in both ApoE-knockout and LDLR-knockout mice aggravates atherosclerosis development [12, 13]. These combined data suggested a main anti-atherogenic role of SRB1 by mediating a crucial step in reverse cholesterol transport. However, it should be noted that ablation of SRB1 in both $ApoE^{-/-}$ and $LDLR^{-/-}$ mice assessed the role of this HDL receptor in absence of physiological catabolism of (V)LDL by the ApoE-LDLR clearance pathway.

Since hepatic SRB1-mediated cholesterol clearance may thus contribute to the atheroprotective effects of brown fat activation, the aim of this study was to evaluate whether knocking down hepatic SRB1 attenuates the therapeutic effectiveness of brown fat activation on atherosclerosis development. To this end, *E3L.CETP* mice, a well-established model of human-like lipoprotein metabolism with an intact ApoE-LDLR pathway for (V)LDL clearance, received a short hairpin RNA (shRNA) targeting SRB1, as delivered by adeno-associated virus serotype 8 (AAV8) that has been widely used to transduce hepatocytes [14, 15]. The effects of knocking down SRB1 on the beneficial effects of β3-AR agonism on lipoprotein metabolism and atherosclerosis development were evaluated.

Materials and methods

Additional detailed materials and methods are included in the **Supplemental methods**.

Animals and treatments

Hemizygous *APOE*3-Leiden* (*E3L*) mice were crossbred with homozygous human cholesteryl ester transfer protein (CETP) transgenic mice to generate heterozygous *E3L.CETP* mice [16]. Please see **the Major Resources Table** in the Supplemental Materials. Mice were housed in

standard conditions at room temperature (22°C) with 40 ± 5% relative humidity and a 12-h light/dark (7 am lights on; 7 pm lights off) cycle. Water and standard laboratory diet (801203, Special Diets Services, UK) were available *ad libitum*, unless indicated.

In a first experiment, 9-12 weeks old female mice were fed a Western-type diet (WTD; Altromin, Germany) containing 15% cacao butter, 1% corn oil and 0.15% (wt/wt) cholesterol. After a run-in period of 3 weeks, mice were randomized into two groups based on plasma lipid levels and body weight and received an injection via the tail vein with an AAV8 vector loaded with shRNA targeting SRB1 (Vector Biolabs, USA, 5×10^{11} genome copies/mouse) or saline as control. 2 weeks after injection, mice in each group were again randomized based on plasma lipid levels and body weight into two subgroups and additionally treated with the β3-AR agonist CL316,243 (Tocris Bioscience Bristol, United Kingdom; 20 μg·mouse^{-1}) or vehicle (saline) 3 times per week by subcutaneous injections between 13:00 and 15:00 h for additional 9 weeks to evaluate atherosclerosis development. This resulted in the following four treatment groups (n=11 mice per group): (i) vehicle (ctrl), (ii) CL316,243 (β), (iii) shSRB1 treatment (shSRB1), (iv) shSRB1 treatment + CL316,243 (shSRB1+β). Body weight and plasma lipid levels were measured at the indicated time points throughout the intervention period. Blood samples for LPL activity assay (see below) were collected after 8 weeks of vehicle or CL316,243 treatment. After 9 weeks of treatment, plasma ApoA1 and CETP levels were measured as described below. VLDL clearance was assessed (see below) and mice were euthanized by CO_2 suffocation and perfused with ice-cold saline via the heart. Organs were isolated for Western blotting and other analysis.

To rule out an effect of the AAV vector itself on plasma lipids, in a second experiment, 9-12 weeks-old female mice were again fed the WTD. After a run-in period of 3 weeks, mice were randomized into three groups based on plasma lipid levels and body weight and received an injection into the tail vein with an AAV8 vector loaded with shRNA targeting SRB1 (shSRB1, Vector Biolabs, USA, 5×10^{11} genome copies/mouse) or with a scrambled sequence (scrambled, Vector Biolabs, USA, 5×10^{11} genome copies/mouse), or saline (ctrl). Body weight was determined every two weeks and plasma lipids were measured after 2 and 6 weeks of treatment.

The set-up of the third experiment was similar to that of the first experiment, with the exception that mice were treated with CL316,243 or vehicle for 4 instead of 9 weeks. At the end of treatment, *in vivo* plasma decay and hepatic uptake of HDL-cholesteryl oleyl ether was measured as described below.

Our study adhered to the guidelines as described in the ATVB Council Statement for considering "sex difference" as a biological variable [17]. We used female mice because only female *E3L.CETP* mice develop WTD-induced dyslipidemia and atherosclerosis [7, 18-20]. Our study also adhered to the guidelines for experimental atherosclerosis studies described in the AHA Statement [21]. The animal experiment was approved by the Animal Ethical Committee of Leiden University Medical Center, Leiden, The Netherlands (AVD1160020173305, PE.18.034.019, PE. 18. 034. 049). All animal procedures performed conform to the guidelines from Directive 2010/63/EU of the European Parliament on the protection of animals used for scientific purposes.

Statistical analysis

Interaction between treatment and genotype and difference between two groups were determined using two-way analysis of variance (ANOVA) followed by a Fisher's LSD post hoc test without testing normality and variance. Difference between two groups in

Supplemental Figure IV was determined using one-way analysis of variance (ANOVA) with the *LSD post hoc* test if F achieved statistical significance ($P < 0.05$) and significant variance inhomogeneity was not observed. The square root (SQRT) of the lesion area was transformed and univariate regression of analyses was performed to test for significant correlations between atherosclerotic lesion area and plasma non-HDL-C/HDL-C/TG exposure. Multiple regression analysis was performed to predict the contribution of plasma non-HDL-C/HDL-C/TG exposure to the atherosclerotic lesion area. Probability values less than 0.05 were considered statistically significant. All statistical analyses were performed with the GraphPad Prism 8.0.1 for Windows except for univariate and multiple regression analyses which were performed with SPSS 25 for Windows.

Results

Hepatic SRB1 knockdown increases HDL-C and decreases non-HDL-C, and additively improves β3-AR agonism-induced reduction in plasma non-HDL-C and increase in HDL-C levels

In a first experiment, to investigate the role of hepatic SRB1 in the beneficial effects of brown fat activation on cholesterol metabolism and atherosclerosis development, *E3L.CETP* mice were injected with shRNA-loaded AAV8 to downregulate liver-specific expression of SRB1 [15]. Hepatic SRB1 was downregulated by approx. 40-55% at both mRNA and protein level as compared to control mice, as assessed after 11 weeks of injection upon termination (**Table 1; Supplemental Figure IA, B**). shSRB1-AAV8 did not reduce SRB1 protein levels in both adrenal glands and gonadal white adipose tissues (gWAT; **Supplemental Figure IE, F**), while it increased SRB1 protein levels in descending thoracic aortas (+48%, **Supplemental Figure IG**). SRB1 knockdown had no effect on the hepatic expression of other genes related to HDL metabolism, including *Apoa1, Abca1, Abcg1,* and *Lcat* (**Table 1**).

2 weeks after shSRB1-AAV8 injection, both control and SRB1 knockdown mice were treated with vehicle or the β3-AR agonist CL316,243 to activate brown fat. β3-AR agonism prevented body weight gain, and decreased gonadal white adipose tissue (gWAT) and intrascapular brown adipose tissue (iBAT) mass in control mice, which is in line with our previous observations [7], confirming the beneficial effects of β3-AR agonism on adiposity, and which was also observed in hepatic SRB1 knockdown mice (**Supplemental Figure IIA-C**). Hepatic SRB1 knockdown *per se* had no effects on adiposity (**Supplemental Figure IIA-C**).

We next explored the effects of hepatic SRB1 knockdown on the plasma lipid-modulating effects of brown fat activation. First, we showed that SRB1 knockdown in control mice increased plasma ApoA1 (+31%, shSRB1 vs. ctrl, **Supplemental Figure IIIA**) and HDL-C levels (**Figure 1A, 1G**), as well as HDL-C exposure (+31%, shSRB1 vs. ctrl, **Figure 1B**), confirming the role of hepatic SRB1 in HDL metabolism. β3-AR agonism in control mice increased plasma HDL-C levels (**Figure 1A, 1G**) and HDL-C exposure (+36%, β vs. ctrl, **Figure 1B**) without effects on plasma ApoA1 levels (**Supplemental Figure IIIA**). Two-way ANOVA analysis revealed that there was no interaction effect between genotype and treatment on HDL-C exposure (two-way ANOVA, $P=0.840$ for genotype × treatment). Thus, in hepatic SRB1 knockdown mice, β3-AR agonism still increased HDL-C levels (**Figure 1A, 1G**) and HDL-C exposure (+21%, shSRB1+ β vs. β; +26%, shSRB1+ β vs. shSRB1; **Figure 1B**).

As expected, β3-AR agonism reduced plasma total cholesterol (TC) levels (**Figure 1C**), resulting in reduced TC exposure (-18%, β vs. ctrl, **Figure 1D**). Interestingly, hepatic SRB1 knockdown *per se* also decreased plasma TC levels (**Figure 1C**) and TC exposure (-15%,

shSRB1 vs. ctrl, **Figure 1D**) as compared to vehicle-treated control mice, and in SRB1 knockdown condition, β3-AR agonism still reduced plasma TC levels (**Figure 1C**) and TC exposure (-14%, shSRB1+β vs. shSRB1, **Figure 1D**). The reduced TC by β3-AR agonism was attributed to non-HDL-C in both control mice (-21%, β vs. ctrl) and SRB1 knockdown mice (-19%, shSRB1+β vs. shSRB1; **Figure 1E-1G**). In addition, SRB1 knockdown additively improved non-HDL-C-lowering effects of β3-AR agonism (-15%, shSRB1+β vs. β; -19%, shSRB1+ β vs. shSRB1; **Figure 1E-1G**). Taken together, both brown fat activation and hepatic SRB1 knockdown in *E3L.CETP* mice improve dyslipidemia by reducing plasma non-HDL-C levels and increasing HDL-C levels, without significant interaction between brown fat activation and hepatic SRB1 knockdown.

Table 1. Hepatic gene expression

	Gene	ctrl	**β**	shSRB1	shSRB1+β
HDL formation and processing	*Apoa1*	1.00 ± 0.09	0.96 ± 0.12	1.24 ± 0.08	1.07 ± 0.10
	Abca1	1.00 ± 0.05	0.89 ± 0.04	1.03 ± 0.03	0.98 ± 0.04
	Abcg1	1.00 ± 0.06	0.91 ± 0.06	0.98 ± 0.04	**0.72 ± 0.02**$^{\#\#\#\$\$}$
	CETP	1.00 ± 0.06	0.87 ± 0.11	1.01 ± 0.05	**0.67 ± 0.09**$^{\#\#}$
	Lcat	1.00 ± 0.08	0.86 ± 0.04	0.92 ± 0.04	0.93 ± 0.03
VLDL production and secretion	*Apob*	1.00 ± 0.05	0.91 ± 0.05	0.97 ± 0.02	0.98 ± 0.05
	Mttp	1.00 ± 0.07	1.10 ± 0.08	1.01 ± 0.03	**1.26 ± 0.07**$^{\#\#}$
	Srebp1c	1.00 ± 0.05	1.01 ± 0.08	1.10 ± 0.07	1.24 ± 0.08
Lipolytic processing	*Lpl*	1.00 ± 0.10	1.12 ± 0.12	0.94 ± 0.07	0.92 ± 0.06
	Hl	1.00 ± 0.06	0.88 ± 0.04	0.86 ± 0.05	0.89 ± 0.06
	Angptl4	1.00 ± 0.08	1.17 ± 0.11	1.05 ± 0.06	1.39 ± 0.19
	Apoc2	1.00 ± 0.04	**1.18 ± 0.08***	1.09 ± 0.05	**1.39 ± 0.07**$^{\#\#}$
Hepatic uptake of cholesterol	*Ldlr*	1.00 ± 0.07	**0.75 ± 0.05****	1.09 ± 0.05	**0.79 ± 0.06**$^{\#\#\#}$
	Lrp1	1.00 ± 0.08	**0.71 ± 0.05*****	**0.70 ± 0.05*****	**0.54 ± 0.04**$^{\$\$}$
	Srb1	1.00 ± 0.07	0.99 ± 0.07	**0.49 ± 0.05*****	**0.59 ± 0.06**$^{\$\$\$}$
	Pcsk9	1.00 ± 0.21	**0.59 ± 0.13***	1.02 ± 0.19	**0.39 ± 0.07****$^{\$\$}$

Values are expressed as mean fold change ± SEM. n= 10/11 mice per group. *P<0.05, **P<0.01, ***P<0.001 vs. ctrl; $^{\$\$}$P<0.01, $^{\$\$\$}$P<0.001 vs **β**; $^{\#\#}$P<0.01, $^{\#\#\#}$P<0.001 vs. shSRB1.

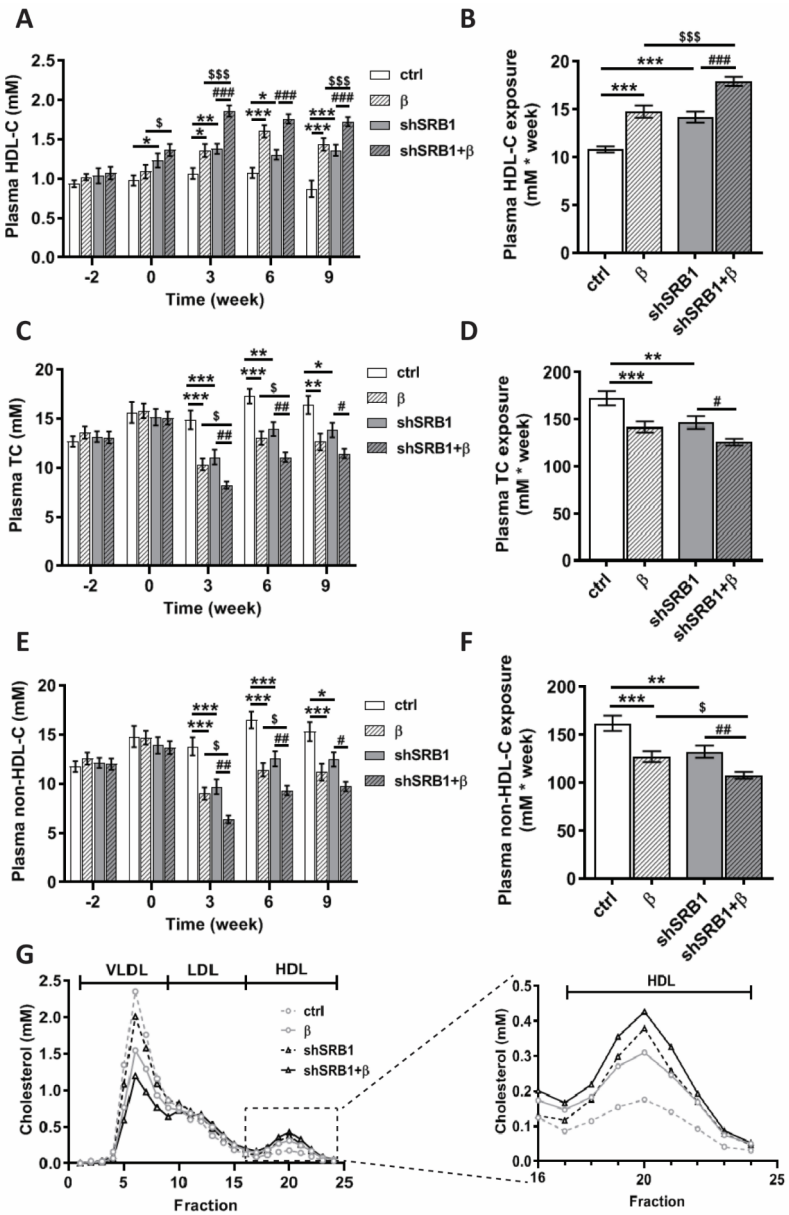

Figure 1. Hepatic SRB1 knockdown increases HDL-C and decreases non-HDL-C, and additively improves β3-AR agonism-induced reduction in plasma non-HDL-C and increase in HDL-C levels. *E3L.CETP* mice fed a WTD and pretreated with vehicle (ctrl) or an adeno-associated virus serotype 8 loaded with an shRNA targeting SRB1 (shSRB1) at week -2, were treated with vehicle or the β3-AR agonist CL316,243 (β) from week 0 for 9 weeks. Plasma samples were collected at indicated time points to determine plasma levels of (**A**) HDL cholesterol (-C), (**C**) total cholesterol (TC), and (**E**) non-HDL-C. (**B**) Plasma HDL-C exposure, (**D**) plasma TC exposure, and (**F**) plasma non-HDL-C exposure were calculated accordingly. (n= 10/11 mice per group) (**G**) Plasma samples obtained at 9 weeks were pooled per group to determine cholesterol distribution over lipoproteins. Values are means ± SEM. Differences

between two groups were determined using two-way ANOVA followed by a Fisher's LSD post hoc test. *P<0.05, **P<0.01, ***P<0.001 vs. ctrl; $^{\$}$P<0.05, $^{\$\$\$}$P<0.001 vs. β; $^{\#}$P<0.05, $^{\#\#}$P<0.01, $^{\#\#\#}$P<0.001 vs. shSRB1.

Hepatic SRB1 knockdown decreases plasma triglycerides, and additively improves β3-AR agonism-induced reduction in plasma triglyceride levels

β3-AR agonism reduced plasma triglyceride (TG) levels (**Figure 2A**) and TG exposure (-34%, β vs. ctrl; **Figure 2B**). Notably, hepatic SRB1 knockdown *per se* also decreased plasma TG levels (**Figure 2A**) and TG exposure (-29%, shSRB1 vs. ctrl; **Figure 2B**). Under condition of hepatic SRB1 knockdown, β3-AR agonism still reduced plasma TG levels (**Figure 2A**) and TG exposure (-23%; **Figure 2B**), although there was a marginal interaction effect of hepatic SRB1 knockdown on TG-lowering effects of β3-AR agonism (two-way ANOVA, P=0.036 for genotype × treatment). TG distribution over lipoproteins revealed that the reduced TG was mainly confined to VLDL (**Figure 2C**). In control mice, β3-AR agonism did not affect the hepatic expression of genes related to VLDL production (i.e. *Apob*, *Srebp1c*, and *Mttp*). In SRB1 knockdown mice, β3-AR agonism did not affect the expression of *Apob* and *Srebp1c*, while increasing *Mttp* expression (+25%, shSRB1+β vs. shSRB1; **Table 1**).

To exclude an effect of the AAV8 vector *per se* on plasma lipids, in a second experiment we treated an additional group of mice with an AAV8 loaded with a scrambled shRNA sequence (scrambled). Indeed, after 6 weeks of treatment, scrambled-AAV8 did not induce any significant effects on body and liver weight or plasma lipid levels, while we again observed that shSRB1-AAV8 increased plasma HDL-C levels (+30%, shSRB1 vs. ctrl; +50%, shSRB1 vs. scrambled) and reduced plasma levels of TC (-20%, shSRB1 vs. ctrl; -25%, shSRB1 vs. scrambled), non-HDL-C (-25%, shSRB1 vs. ctrl; -31%, shSRB1 vs. scrambled) and TG (-40%, shSRB1 vs. ctrl; -40%, shSRB1 vs. scrambled) (**Supplemental Figure IV C-F**).

β3-AR agonism did not influence hepatic gene expression of hepatic lipase (*Hl*), lipoprotein lipase (*Lpl*) and *Angptl4*, but increased *Apoc2* expression in both control (+19%, β vs. ctrl) and SRB1 knockdown mice (+27%; shSRB1+β vs. shSRB1; **Table 1**), which may imply that β3-AR agonism increases endogenous LPL activity. Indeed, post-heparin plasma was collected after 8 weeks of vehicle or CL316,243 treatment to show that β3-AR agonism increased total endogenous LPL activity in both control mice (+84%, β vs. ctrl) and shSRB1 knockdown mice (+76%, shSRB1+β vs. ctrl), without effects on endogenous HL activity (**Figure 2D**). SRB1 knockdown *per se* did not influence HL or LPL activity (**Figure 2D**). Together, these data show that brown fat activation in *E3L.CETP* mice reduces plasma TG related to enhanced endogenous LPL activity, both of which were not influenced by hepatic SRB1 knockdown.

Hepatic SRB1 knockdown on top of β3-AR agonism increases VLDL surface phospholipid transfer and VLDL clearance, without affecting kinetics of HDL cholesteryl ether

Next, we investigated the effect of SRB1 knockdown in combination with β3-AR agonism on plasma VLDL catabolism by injection of VLDL-mimicking particles [22] that were double-labeled with [^{3}H]DPPC (*i.e.* surface marker) and [^{14}C]CO (*i.e.* core marker). β3-AR agonism accelerated [^{3}H]DPPC clearance from the circulation in control and SRB1 knockdown mice (**Figure 3A**). β3-AR agonism increased total activity of [^{3}H]DPPC transferred to HDL in SRB1 knockdown mice as an indication of increased surface phospholipid transfer to HDL, while no effect was observed in control mice (**Figure 3B**). In addition, β3-AR agonism increased the ratio of [^{3}H]DPPC in HDL over non-HDL in both control and SRB1 knockdown *E3L.CETP* mice (**Figure 3C**).

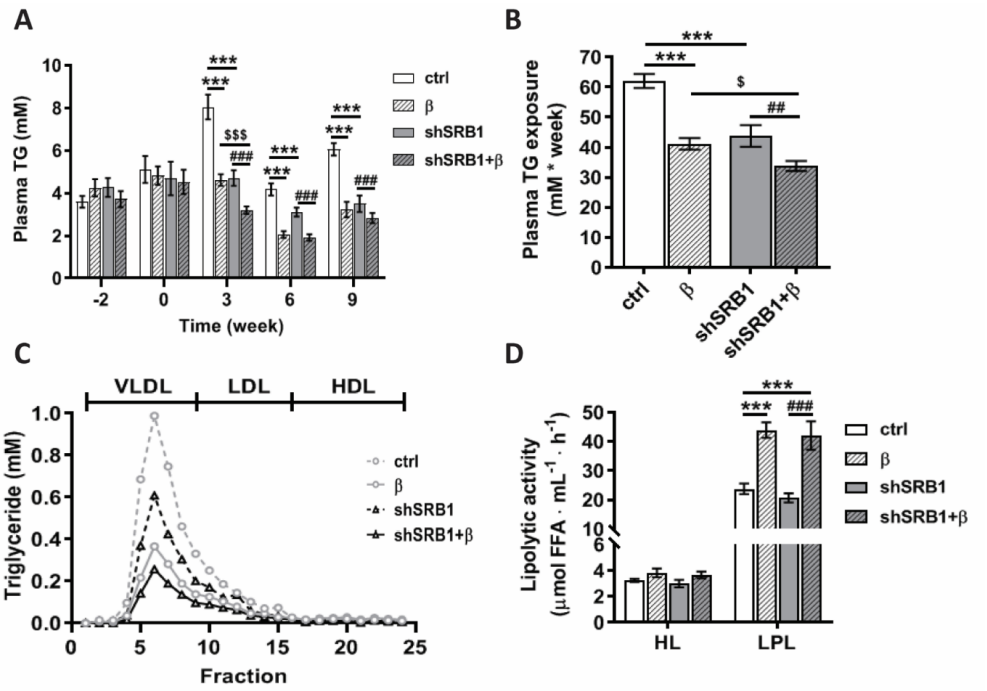

Figure 2. Hepatic SRB1 knockdown decreases plasma triglycerides, and additively improves β3-AR agonism-induced reduction in plasma triglyceride levels. *E3L.CETP* mice fed a WTD and pretreated with vehicle (ctrl) or an adeno-associated virus serotype 8 loaded with an shRNA targeting SRB1 (shSRB1) at week -2, were treated with vehicle or the β3-AR agonist CL316,243 (β) from week 0 for 9 weeks. Plasma samples were collected at indicated time points to determine (**A**) plasma triglyceride (TG) levels and (**B**) plasma TG exposure. (n= 10/11 mice per group) (**C**) Plasma samples at 9 week were pooled per group to determine TG distribution over lipoproteins. (**D**) after 8 weeks of vehicle or CL316,243 treatment mice were intravenously injected with heparin. Before and 10 min after injection plasma was collected. Endogenous hepatic lipase (HL) and lipoprotein lipase (LPL) activity was determined using a substrate mixture containing glycerol tri[^{3}H]oleate-labeled VLDL-like particles in the presence or absence of 1 M NaCl which inhibits LPL activity. (n= 10/11 mice per group) Values are means ± SEM. Differences between two groups were determined using two-way ANOVA followed by a Fisher's LSD post hoc test. ***P<0.001 vs. ctrl; $^{\$}$P<0.05, $^{\$\$\$}$P<0.001 vs. β; $^{\#\#}$P<0.01, $^{\#\#\#}$P<0.001 vs. shSRB1.

Although β3-AR agonism and hepatic SRB1 knockdown downregulated hepatic LDL receptor (*Ldlr*) and LDLR related protein 1 (*Lrp1*) expression (**Table 1**), combination treatment increased LDLR protein levels (**Supplemental Figure IA, C, D**). β3-AR agonism increased [^{14}C]CO clearance from the circulation (**Figure 3D**) and increased uptake of [^{14}C]CO by the liver in both control mice (+26%, β vs. ctrl) and SRB1 knockdown mice (+28%, shSRB1+β vs. shSRB1; **Figure 3E**). SRB1 knockdown combined with β3-AR agonism further increased plasma clearance (**Figure 3D**) and tended to further increase hepatic uptake of [^{14}C]CO (P=0.078, +18%, shSRB1+ β vs. β; **Figure 3E**).

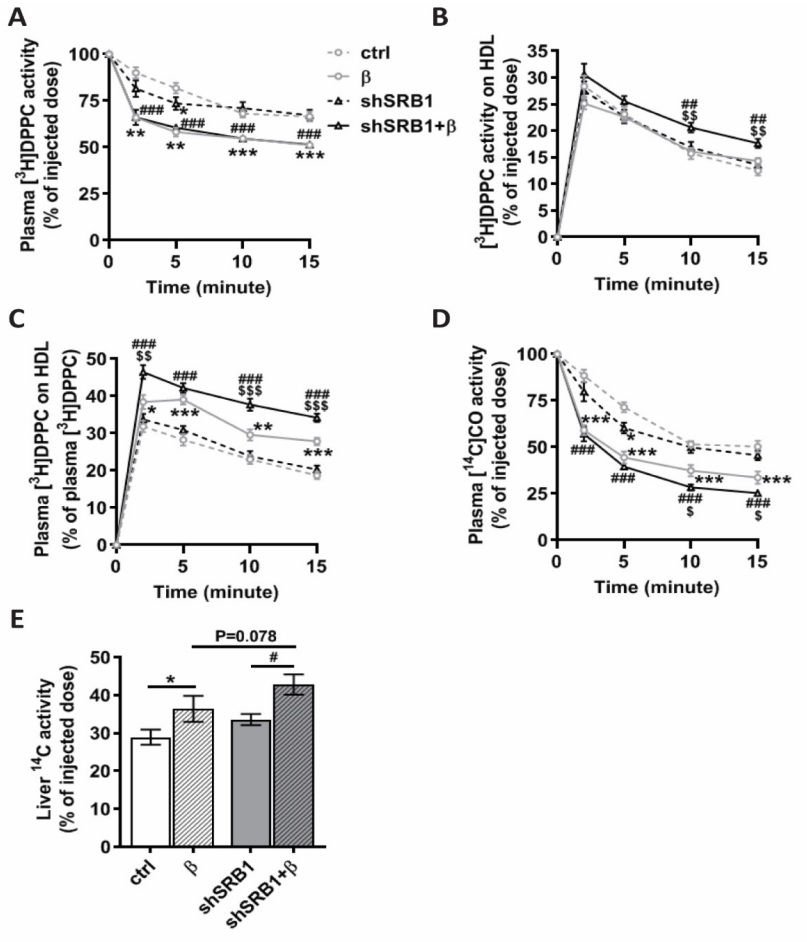

Figure 3. Hepatic SRB1 knockdown on top of β3-AR agonism increases VLDL surface phospholipid transfer and VLDL clearance. *E3L.CETP* mice fed a WTD and pretreated with vehicle (ctrl) or an adeno-associated virus serotype 8 loaded with an shRNA targeting SRB1 (shSRB1) at week -2, were treated with vehicle or the β3-AR agonist CL316,243 (β) from week 0. At week 9, mice were intravenously injected with [^{3}H]dipalmitoylphosphatidylcholine (DPPC) and [^{14}C]cholesteryl oleate ([^{14}C]CO) doubly labelled VLDL-mimicking particles. Plasma samples were collected at indicated time points and clearance of (**A**) [^{3}H]DPPC and (**D**) [^{14}C]CO was determined. HDL was isolated to determine (**B**) [^{3}H]DPPC activities on HDL and (**C**) ratio of [^{3}H]DPPC activity of HDL over non-HDL. (**E**) Hepatic uptake of [^{14}C]CO was measured after 15 min of particle injection. (n= 10/11 mice per group) Values are means ± SEM. Differences between two groups were determined using two-way ANOVA followed by a Fisher's LSD post hoc test. *P<0.05, **P<0.01, ***P<0.001 vs. ctrl; $^{\$}$P<0.05, $^{\$\$}$P<0.01, $^{\$\$\$}$P<0.001 vs. β; $^{\#}$P<0.05, $^{\#\#}$P<0.01, $^{\#\#\#}$P<0.001 vs. shSRB1.

Since it is possible that HDL-cholesteryl esters could be transferred to (V)LDL in the presence of CETP and subsequently taken up by the liver to contribute the cholesterol-lowering effects of hepatic SRB1 knockdown, we determined the effects of the various treatments on hepatic *CETP* expression and plasma CETP levels. While the combination treatment decreased hepatic *CETP* expression, hepatic SRB1 knockdown, β3-AR agonism and the combination did not influence plasma CETP levels (**Supplemental Figure IIIB**) or plasma decay and hepatic uptake of HDL-cholesteryl oleyl ether (**Supplemental Figure VA, B**).

Collectively, these data suggest that hepatic SRB1 knockdown increases plasma HDL as avid acceptor of VLDL-derived surface remnants, which accelerates LPL-mediated VLDL lipolysis and subsequent hepatic uptake of VLDL core remnants.

Hepatic SRB1 knockdown additively improves β3-AR agonism**-induced attenuation in atherosclerosis development**

After 9 weeks of hepatic SRB1 knockdown combined with β3-AR agonism, atherosclerosis development was evaluated. The aortic roots of the hearts were isolated and stained to evaluate atherosclerotic lesion area and severity. β3-AR agonism markedly reduced atherosclerotic lesion area through the aortic root (**Figure 4A, 4B**), resulting in lower mean atherosclerotic lesion area (-38%, β vs. ctrl; **Figure 4C**). Hepatic SRB1 knockdown *per se* also clearly reduced atherosclerotic lesion area (-42%, shSRB1 vs. ctrl; **Figure 4A-C**) and lesion severity (**Figure 4A, 4D**) as compared to vehicle-treated control mice. SRB1 knockdown did not abrogate β3-AR agonism induced attenuation in atherosclerotic lesion area (two-way ANOVA, P=0.402 for genotype × treatment). Rather, β3-AR agonism in SRB1 knockdown mice further reduced lesion area (-43%, shSRB1+ β vs. β; -39%, shSRB1+ β vs. shSRB1; **Figure 4A-4C**). We further analyzed association between plasma lipid exposure and atherosclerosis development. Non-HDL-C exposure (R^2=0.315, P<0.0001; **Figure 4E**), HDL-C exposure (R^2=0.190, P=0.004; **Figure 4F**), and TG exposure (R^2=0.202, P=0.003; **Figure 4G**) were all associated with the square root (SQRT) of atherosclerotic lesion area, indicating all these factors contributed to the reduced atherosclerosis development.

Finally, we characterized atherosclerotic lesion composition by analyzing the relative plaque content of smooth muscle cells (SMC), collagen, and macrophages. β3-AR agonism and SRB1 knockdown *per se*, as well as their combination had no significant effect on lesion composition including SMCs, collagen, and macrophages (**Figure 5A-D, Supplemental Figure VI**), and did not affect the ratio of stable markers (i.e. SMC and collagen area) versus the unstable marker (i.e. macrophage area) (**Figure 5E**). β3-AR agonism under the condition of SRB1 knockdown increased the ratio of SMC and collagen area versus macrophage area (+28%, shSRB1+ β vs. β; **Figure 5E**).

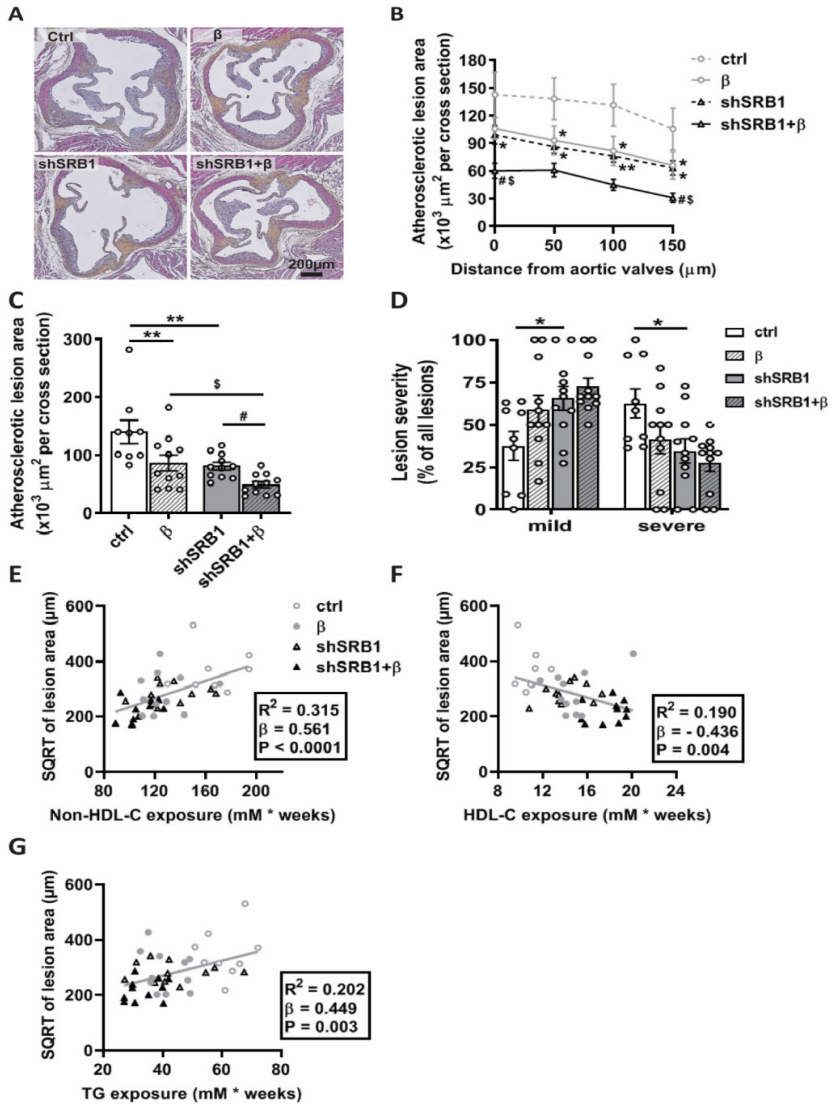

Figure 4. Hepatic SRB1 knockdown additively improves β3-AR agonism-induced attenuation in atherosclerosis development. *E3L.CETP* mice fed a WTD and pretreated with vehicle (ctrl) or an adeno-associated virus serotype 8 loaded with an shRNA targeting SRB1 (shSRB1) at week -2, were treated with vehicle or the β3-AR agonist CL316,243 (β) from week 0 for 9 weeks. (**A**) Hearts were collected and cross-sections of the aortic roots were stained with hematoxylin-phloxine-saffron and representative pictures of atherosclerotic lesions of each group are presented. (**B**) Plaque lesion area as a function of distance from the appearance of open valves and (**C**) mean atherosclerotic lesion area were calculated. (**D**) Lesions were categorized according to lesion severity. The square root (SQRT) of the mean atherosclerotic lesion area was plotted against the plasma (**E**) non-HDL cholesterol (-C) exposure, (**F**) HDL-C exposure, and (**G**) TG exposure. (n= 7 - 11 mice per group) Values are means ± SEM. Differences between two groups were determined using two-way ANOVA followed by a Fisher's LSD post hoc test. *P<0.05, **P<0.01 vs. ctrl; $P<0.05 vs. β; #P<0.05 vs. shSRB1.

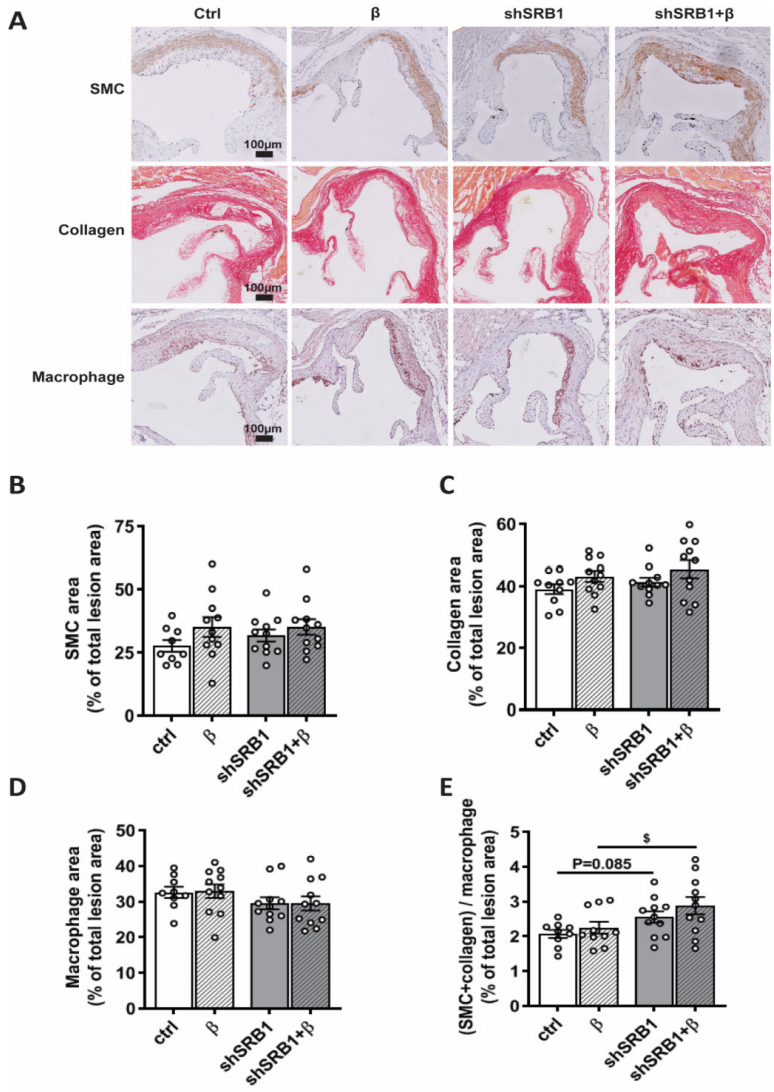

Figure 5. Hepatic SRB1 knockdown on top of β3-AR agonism increases the ratio of smooth muscle cell and collagen area to macrophage area. *E3L.CETP* mice fed a WTD and pretreated with vehicle (ctrl) or an adeno-associated virus serotype 8 loaded with an shRNA targeting SRB1 (shSRB1) at week -2, were treated with vehicle or the β3-AR agonist CL316,243 (β) from week 0 for 9 weeks. Cross-sections of aortic root were stained for (**A, B**) smooth muscle cells (SMC), (**A, C**) collagen and (**A, D**) macrophages, and their relative areas within the lesions were quantified. (**E**) The ratio of SMC area and collagen area to macrophage area was calculated. (n= 9/11 mice per group) Values are means ± SEM. Differences between two groups were determined using two-way ANOVA followed by a Fisher's LSD post hoc test. $^{\$}$P<0.05 vs. β.

Discussion

Previously we demonstrated that brown fat activation by β3-AR agonism reduced atherosclerosis development, which could be explained by both LDLR-dependent hepatic clearance of TRL remnants [7] and increased SRB1-mediated reverse cholesterol transport [8]. While previous studies have demonstrated the crucial role of the ApoE-LDLR pathway in the antiatherogenic effects of brown fat activation [7, 23], the specific role of hepatic SRB1 in the antiatherogenic effect of brown fat activation was still obscure. By using the *E3L.CETP* mouse model, we now demonstrated that hepatic SRB1 knockdown in the presence of an intact ApoE-LDLR clearance pathway for TRL remnants did not attenuate the anti-atherogenic effects of β3-AR activation. Rather, hepatic SRB1 knockdown *per se* appeared to improve hyperlipidaemia and consequently reduce atherosclerosis development.

First, we showed that partial knockdown of hepatic SRB1 (40-50%) in E3L.CETP mice increases HDL-C as well as ApoAI without an obvious increase in HDL size, indicating an increase in HDL pool size [24], and does not affect the clearance of [^{3}H]COEth-HDL from plasma. This may be somewhat counterintuitive, since SRB1-deficiency on a wild-type background largely increases HDL size in addition to increased HDL-C, and delays plasma clearance of [^{3}H]COEth-HDL [25]. It should, however, be noted we previously also showed that crossbreeding of SRB1-deficient mice with CETP-transgenic mice largely prevents the increase in HDL size as well as the delay in plasma decay of [^{3}H]COEth-HDL resulting from SRB1-deficiency, while HDL-C was still increased, in mice fed a Western-type diet [25]. These findings can be explained by CETP-mediated transfer of HDL-CE to apoB-containing particles, which prevents CE accumulation in HDL and thereby prevents an obvious increase in HDL size, at least judged from FPLC profiling, as well as a delay in HDL-CE clearance. Nevertheless, the precise reason for the increase in ApoAI, as thus HDL pool size, is still unclear and deserves attention in future research.

Hepatic SRB1 knockdown also caused a striking reduction in TG and cholesterol within non-HDL. This may seem surprising given previous findings suggesting that SRB1 facilitates hepatic TRL remnant uptake [26]. Likely, the increased HDL resulting from SRB1 knockdown forms a larger pool of acceptors for TRL surface remnants generated during LPL-mediated lipolysis of VLDL, as we showed by increased transfer of TRL-derived phospholipids to HDL. As a consequence, lipolytic TRL processing is accelerated followed by avid hepatic clearance of TRL remnants via the ApoE-LDLR pathway in *E3L.CETP* mice. Apparently, this effect occurs under conditions of unchanged endogenous lipolytic activity. At the same the time, in *E3L.CETP* mice the build-up of cholesterol in HDL induced by partial hepatic SRB1-knockdown can be partially relieved by CETP-mediated transfer of HDL-associated cholesteryl esters to TRL with subsequent clearance via the ApoE-LDLR pathway [27]. This may explain why plasma clearance and hepatic uptake of HDL-cholesteryl ether was not influenced by hepatic SRB1 knockdown. In line with our findings, a genetic variant (P297S) of SCARB1, the gene encoding SRB1 in humans also tended to decrease VLDL-C (-44%, P=0.07) besides raising HDL-C as compared to family controls [28], and a more recent meta-analysis showed that the SCARB1 rs5888 polymorphism associates with lower plasma TG levels besides higher HDL-C in men [29]. Collectively, our data confirm the relevance of our mouse model for human-like lipid metabolism, and are consistent with the notion that hepatic SRBI knockdown improves TRL metabolism in the presence of an intact ApoE-LDLR clearance pathway.

Furthermore, we observed that hepatic SRB1 knockdown attenuated atherosclerosis development in *E3L.CETP* mice. Recently, Huang *et al.* reported that endothelial cell-specific

SRB1 deficiency in ApoE$^{-/-}$ mice protects against atherosclerosis development, via blocking endothelial LDL transcytosis without effects on plasma TC, TG and HDL levels [30]. Such a mechanism seems unlikely to explain the reduction in atherosclerosis observed in our model, as shSRB1-AAV8 specifically downregulated SRB1 expression in the liver, and even increased SRB1 protein levels in aortas. At first glance, the reduction of atherosclerosis induced by selective hepatic SRB1 knockdown may seem surprising given that SRB1-deficiency aggravated atherosclerosis development in ApoE$^{-/-}$ mice [12] and in LDLR$^{-/-}$ mice, without lowering non-HDL-C [13]. Likely, these opposing effects of SRB1 on atherosclerosis are explained by the difference in genetic backgrounds between these disease models. As the hepatic ApoE-LDLR clearance pathway for TRL remnants is absent in both ApoE$^{-/-}$ and LDLR$^{-/-}$ mice, SRB1 deficiency does not reduce non-HDL-C and the increased atherosclerosis is likely explained by increased oxidative stress [25]. In favourable contrast, *E3L.CETP* mice have an intact ApoE-LDLR clearance pathway and CETP, which facilitate hepatic clearance of cholesterol from TRL remnants and indirectly from HDL, thereby lowering non-HDL-C-induced atherosclerosis development. In support of our findings, inhibition of hepatic SRB1 by RNA interference also attenuated atherosclerosis in rabbits, an animal model that naturally expresses CETP [31]. Although a rare variant in SCARB1 has been reported to increase the risk for coronary heart disease [32], studies investigating other SCARB1 mutations did not show either increased atherosclerosis or CAD [28, 33]. As large-scale human studies addressing the role of SRB1 in cardiovascular disease are still lacking, the jury on the precise role of SRB1 is still out. Based on our study in *E3L.CETP* mice and previous observations in rabbits, loss-of-function SCARB1 mutations in humans may in fact slow down atherosclerosis progression and could in fact be cardioprotective.

Given that SRB1 deficiency in *E3L.CETP* mice reduces non-HDL-C and attenuates atherosclerosis progression, it is not surprising that SRB1 deficiency improved the atheroprotective effects of brown fat activation by β3-AR agonism. Previously, we demonstrated that brown fat activation protects against atherosclerosis development, which was largely due to accelerated TRL remnant clearance via the ApoE-LDLR pathway [7]. Since SRB1 knockdown apparently evoked the same effect, the combined effect of β3-AR agonism and SRB1 knockdown was an additive reduction in non-HDL-C, which can be further explained since combination treatment resulted in higher hepatic LDL protein levels likely caused by reduced hepatic *Pcsk9* expression. Given the tight relation between non-HDL-C exposure and lesion size, this translated in an additive reduction in atherosclerosis. In this study, we mainly focused on effects on lipid metabolism, while brown fat activation displays additional benefits, including decreased inflammation [34], decreased oxidative stress [35], and improved glucose metabolism [34, 36]. Further studies will be needed to investigate whether hepatic SRB1 pathway may contribute to those potentially antiatherogenic benefits of brown fat activation.

The findings from the present study are likely of clinical relevance. Brown fat is functional in both healthy and obese individuals [37, 38], long term brown fat activation by cold exposure reduces LDL-C in hypercholesterolemic patients [39] and brown fat activity is associated with a reduced risk of CVD events [40]. A series of studies shows that Mirabegron, a β3-AR agonist clinically approved for the treatment of overactive bladder, induces beiging of subcutaneous white adipose tissue and increases brown fat activity in humans. This results in improvement in glucose homeostasis and increase in whole-body energy expenditure, plasma HDL-C levels, as well as other beneficial metabolic biomarkers [9, 41-44]. Therefore, pharmacological strategies to activate brown fat in humans may prove to reduce CVD risk. Since hepatic SRB1 knockdown apparently does not interfere with the anti-atherogenic effects of brown fat

activation, such pharmacological strategies may be equally effective in those individuals with compromised SRB1 function, which would be subject for future studies.

In conclusion, by using a relevant mouse model for human-like lipoprotein metabolism, *i.e.* with an intact ApoE-LDLR clearance pathway, we showed that hepatic SRB1 knockdown not only increases HDL-C, but also lowers non-HDL-C and attenuates atherosclerosis development. As such, combined brown fat activation and hepatic SRB1 knockdown additively improve the anti-atherogenic properties of brown fat activation.

Acknowledgments

This work was supported by the Netherlands Organisation for Scientific Research-NWO (VENI grant 91617027 to Y.W.); the Netherlands Organisation for Health Research and Development-ZonMW (Early Career Scientist Hotel grant 435004007 to Y.W.); the Netherlands Cardiovascular Research Initiative: an initiative with support of the Dutch Heart Foundation (CVON-GENIUS-2 to P.C.N.R.); and the Netherlands Heart Foundation (2009T038 to P.C.N.R.). Y.W. is supported by the China "Thousand Talents Plan" (Yong Talents), Shaanxi province "Thousand Talents Plan" (Young Talents) and Foundation of Xi'an Jiaotong University (Plan A). E.Z. is supported by the China Scholarship Council (CSC, grant 201606010321).

Author contributions

E.Z. designed the study, performed experiments, analyzed the data, and drafted the manuscript; Z.L., H.N., C.L., and Z.Y., contributed to animal experiments. A.C.F., J.F.P.B., and K.W. interpreted data. P.C.N.R. and Y.W. designed the study and revised the manuscript constructively.

Conflict of interest

The authors report no declarations of interest.

References

1. Jukema, J.W., et al., *The controversies of statin therapy: weighing the evidence.* J Am Coll Cardiol, 2012. **60**(10): p. 875-81.
2. Collins, R., et al., *Interpretation of the evidence for the efficacy and safety of statin therapy.* Lancet, 2016. **388**(10059): p. 2532-2561.
3. Cholesterol Treatment Trialists, C., *Efficacy and safety of statin therapy in older people: a meta-analysis of individual participant data from 28 randomised controlled trials.* Lancet, 2019. **393**(10170): p. 407-415.
4. van Dam, A.D., et al., *Targeting white, brown and perivascular adipose tissue in atherosclerosis development.* Eur J Pharmacol, 2017. **816**: p. 82-92.
5. Hoeke, G., et al., *Role of Brown Fat in Lipoprotein Metabolism and Atherosclerosis.* Circ Res, 2016. **118**(1): p. 173-82.
6. Ruiz, J.R., et al., *Role of Human Brown Fat in Obesity, Metabolism and Cardiovascular Disease: Strategies to Turn Up the Heat.* Prog Cardiovasc Dis, 2018. **61**(2): p. 232-245.
7. Berbee, J.F., et al., *Brown fat activation reduces hypercholesterolaemia and protects from atherosclerosis development.* Nat Commun, 2015. **6**: p. 6356.
8. Bartelt, A., et al., *Thermogenic adipocytes promote HDL turnover and reverse cholesterol transport.* Nat Commun, 2017. **8**: p. 15010.
9. O'Mara, A.E., et al., *Chronic mirabegron treatment increases human brown fat, HDL cholesterol, and insulin sensitivity.* J Clin Invest, 2020. **130**(5): p. 2209-2219.
10. Hoeke, G., et al., *Short-term cooling increases serum triglycerides and small high-density lipoprotein levels in humans.* J Clin Lipidol, 2017. **11**(4): p. 920-928 e2.
11. Out, R., et al., *Scavenger receptor class B type I is solely responsible for the selective uptake of cholesteryl esters from HDL by the liver and the adrenals in mice.* J Lipid Res, 2004. **45**(11): p. 2088-95.
12. Braun, A., et al., *Loss of SR-BI expression leads to the early onset of occlusive atherosclerotic coronary artery disease, spontaneous myocardial infarctions, severe cardiac dysfunction, and premature death in apolipoprotein E-deficient mice.* Circ Res, 2002. **90**(3): p. 270-6.
13. Liao, J., et al., *Deficiency of scavenger receptor class B type 1 leads to increased atherogenesis with features of advanced fibroatheroma and expansive arterial remodeling.* Cardiovasc Pathol, 2017. **27**: p. 26-30.
14. van den Hoek, A.M., et al., *APOE*3Leiden.CETP transgenic mice as model for pharmaceutical treatment of the metabolic syndrome.* Diabetes Obes Metab, 2014. **16**(6): p. 537-44.
15. Sands, M.S., *AAV-mediated liver-directed gene therapy.* Methods Mol Biol, 2011. **807**: p. 141-57.
16. Westerterp, M., et al., *Cholesteryl ester transfer protein decreases high-density lipoprotein and severely aggravates atherosclerosis in APOE*3-Leiden mice.* Arterioscler Thromb Vasc Biol, 2006. **26**(11): p. 2552-9.
17. Robinet, P., et al., *Consideration of Sex Differences in Design and Reporting of Experimental Arterial Pathology Studies-Statement From ATVB Council.* Arterioscler Thromb Vasc Biol, 2018. **38**(2): p. 292-303.
18. Landlinger, C., et al., *The AT04A vaccine against proprotein convertase subtilisin/kexin type 9 reduces total cholesterol, vascular inflammation, and atherosclerosis in APOE*3Leiden.CETP mice.* Eur Heart J, 2017. **38**(32): p. 2499-2507.
19. Zadelaar, S., et al., *Mouse models for atherosclerosis and pharmaceutical modifiers.* Arterioscler Thromb Vasc Biol, 2007. **27**(8): p. 1706-21.

20. van Vlijmen, B.J., et al., *Modulation of very low density lipoprotein production and clearance contributes to age- and gender- dependent hyperlipoproteinemia in apolipoprotein E3-Leiden transgenic mice.* J Clin Invest, 1996. **97**(5): p. 1184-92.
21. Daugherty, A., et al., *Recommendation on Design, Execution, and Reporting of Animal Atherosclerosis Studies: A Scientific Statement From the American Heart Association.* Arterioscler Thromb Vasc Biol, 2017. **37**(9): p. e131-e157.
22. Rensen, P.C., et al., *Selective liver targeting of antivirals by recombinant chylomicrons--a new therapeutic approach to hepatitis B.* Nat Med, 1995. **1**(3): p. 221-5.
23. Dong, M., et al., *Cold exposure promotes atherosclerotic plaque growth and instability via UCP1-dependent lipolysis.* Cell Metab, 2013. **18**(1): p. 118-29.
24. Akinkuolie, A.O., et al., *High-density lipoprotein particle subclass heterogeneity and incident coronary heart disease.* Circ Cardiovasc Qual Outcomes, 2014. **7**(1): p. 55-63.
25. Hildebrand, R.B., et al., Restoration of high-density lipoprotein levels by cholesteryl ester transfer protein expression in scavenger receptor class B type I (SR-BI) knockout mice does not normalize pathologies associated with SR-BI deficiency. Arterioscler Thromb Vasc Biol, 2010. 30(7): p. 1439-45.
26. Out, R., et al., *Scavenger receptor BI plays a role in facilitating chylomicron metabolism.* J Biol Chem, 2004. **279**(18): p. 18401-6.
27. Rensen, P.C. and L.M. Havekes, *Cholesteryl ester transfer protein inhibition: effect on reverse cholesterol transport?* Arterioscler Thromb Vasc Biol, 2006. **26**(4): p. 681-4.
28. Vergeer, M., et al., *Genetic variant of the scavenger receptor BI in humans.* N Engl J Med, 2011. **364**(2): p. 136-45.
29. Ye, L.F., et al., *Meta-analysis of the association between SCARB1 polymorphism and fasting blood lipid levels.* Oncotarget, 2017. **8**(46): p. 81145-81153.
30. Huang, L., et al., *SR-B1 drives endothelial cell LDL transcytosis via DOCK4 to promote atherosclerosis.* Nature, 2019. **569**(7757): p. 565-569.
31. Demetz, E., et al., *Inhibition of hepatic scavenger receptor-class B type I by RNA interference decreases atherosclerosis in rabbits.* Atherosclerosis, 2012. **222**(2): p. 360-6.
32. Zanoni, P., et al., *Rare variant in scavenger receptor BI raises HDL cholesterol and increases risk of coronary heart disease.* Science, 2016. **351**(6278): p. 1166-71.
33. Helgadottir, A., et al., *Rare SCARB1 mutations associate with high-density lipoprotein cholesterol but not with coronary artery disease.* Eur Heart J, 2018. **39**(23): p. 2172-2178.
34. Shankar, K., et al., *Role of brown adipose tissue in modulating adipose tissue inflammation and insulin resistance in high-fat diet fed mice.* Eur J Pharmacol, 2019. **854**: p. 354-364.
35. Cai, Y.Y., et al., *Renoprotective effects of brown adipose tissue activation in diabetic mice.* J Diabetes, 2019. **11**(12): p. 958-970.
36. Stanford, K.I., et al., *Brown adipose tissue regulates glucose homeostasis and insulin sensitivity.* J Clin Invest, 2013. **123**(1): p. 215-23.
37. Ouellet, V., et al., *Brown adipose tissue oxidative metabolism contributes to energy expenditure during acute cold exposure in humans.* J Clin Invest, 2012. **122**(2): p. 545-52.
38. Blondin, D.P., et al., *Selective Impairment of Glucose but Not Fatty Acid or Oxidative Metabolism in Brown Adipose Tissue of Subjects With Type 2 Diabetes.* Diabetes,

2015. **64**(7): p. 2388-97.
39. De Lorenzo, F., et al., *Central cooling effects in patients with hypercholesterolaemia.* Clin Sci (Lond), 1998. **95**(2): p. 213-7.
40. Takx, R.A., et al., *Supraclavicular Brown Adipose Tissue 18F-FDG Uptake and Cardiovascular Disease.* J Nucl Med, 2016. **57**(8): p. 1221-5.
41. Finlin, B.S., et al., *The beta3-adrenergic receptor agonist mirabegron improves glucose homeostasis in obese humans.* J Clin Invest, 2020. **130**(5): p. 2319-2331.
42. Finlin, B.S., et al., *Human adipose beiging in response to cold and mirabegron.* JCI Insight, 2018. **3**(15).
43. Baskin, A.S., et al., *Regulation of Human Adipose Tissue Activation, Gallbladder Size, and Bile Acid Metabolism by a beta3-Adrenergic Receptor Agonist.* Diabetes, 2018. **67**(10): p. 2113-2125.
44. Cypess, A.M., et al., *Activation of human brown adipose tissue by a beta3-adrenergic receptor agonist.* Cell Metab, 2015. **21**(1): p. 33-8.

Supplemental appendix

Supplemental materials and methods

Plasma lipid/ApoA1 assays and lipoprotein profiles

At the indicated time points throughout the intervention period, four hour-fasted blood was collected from the tail vein into heparin-coated capillaries that were subsequently placed on ice and centrifuged. Plasma triglyceride (TG) and total cholesterol (TC) levels were measured using enzymatic kits from Roche Diagnostics (Mannheim, Germany). To measure HDL-C, ApoB-containing lipoproteins were precipitated from plasma using 20% polyethylene glycol 6,000 in 200 mM glycine buffer (pH 10). HDL-C was measured in the supernatant as described for TC. Plasma non-HDL-C levels were determined by subtraction of HDL-C from TC levels. Plasma TG, TC and non-HDL-C exposure was calculated as the area under the curve of these plasma lipids during period of vehicle or shSRB1-AAV8 treatment. In the first experiment, after 9 weeks of treatment, 5 µL plasma samples per mouse (n = 10/11 mice per group) were pooled in each treatment group to determine the triglyceride and cholesterol profiles by fast-performance liquid chromatography using a Superose 6 column (GE Healthcare, Piscataway, NJ, USA). A single determination for a group using a pooled plasma sample may provide little or potentially inaccurate information on either of these variables [1]. Plasma ApoA1 levels after 9 weeks of vehicle or CL316,243 treatment in the first experiment were measured using a mouse ApoA1 ELISA kit (ab238260, Abcam) according to the manufacturer's protocol.

Plasma CETP assay

Plasma CETP levels after 9-weeks of vehicle or CL316,243 treatment in the first experiment were measured with an in-house enzyme-linked immune sorbent assay (ELISA) as previously described [2]. Plates (Cat. 442404, Thermo Scientific) were coated with 100 µL TP1 (5 µg/mL, Ottawa Heart Institute Research Cooperation, Canada) and TP2 (2.5 µg/mL, Ottawa Heart Institute Research Cooperation, Canada) antibody mix overnight at 4°C. Plates were then washed and incubated with 1% BSA for 2 h at room temperature. Plates were washed using PBS with 0.1% Triton-X100 and 100 µL diluted plasma samples or standards were added and incubated for 2 h at 37°C. Subsequently, 100 µL detection antibody (0.47 µg/mL anti-TP20 labelled with digoxigenin) (Ottawa Heart Institute Research Cooperation, Canada) was added (2 h at 37°C) followed by 100 µL anti-digoxigenin-POD, Fab fragments coupled to peroxidase (0.0375 U/mL, Roche Molecular Biochemicals, Germany) (1 h at 37°C). The reaction was stopped by adding 100 µL 2 M sulfuric acid and absorbance was measured at 450 nm.

Endogenous LPL activity assay

In the first experiment, after 8 weeks of vehicle or CL316,243 treatment, LPL lipolytic activity was assessed as previously described [3]. Four hour-fasted blood was collected via tail vein before ('pre-heparin') and at 10 min after intravenous injection of heparin (´post-heparin') (0.1 U/g body weight, LEO Pharma B.V., Amsterdam, The Netherlands). Glycerol tri[^{3}H]oleate-labeled VLDL-mimicking particles (80 nm) were prepared as described [4] and incubated (1 mg/mL TG) with 10 µL plasma samples at 37°C in 2% free fatty acid-free BSA, and 0.1 M Tris-HCl pH 8.5 buffer at a total volume of 200 µL. 50 µL of H_2O or NaCl (5 M) was added to determine total lipase (HL + LPL) activity or HL activity (i.e. in presence of NaCl). At t = 30 min and 60 min, 50 µL samples from 260 µL total incubation volume were added to 3.25 mL heptane/ methanol/ chloroform (100:128:137, vol/vol/vol) to terminate lipolysis. 1 mL K_2CO_3 (0.1 M, pH adjusted to 10.5 with saturated boric acid solution) was added to turn liberated [^{3}H] oleate into salt. After vigorous vortexing (10 sec) and centrifugation (15 min at 3600 rpm), ^{3}H radioactivity in 0.5 mL of the aqueous phase was counted and corrected for total aqueous

phase. LPL activity was determined by subtraction of HL activity from total lipase activity (μmol free fatty acids liberated per mL per h) [5].

***In vivo* plasma decay and hepatic uptake of HDL-cholesteryl ether**

[^{3}H]Cholesteryl oleyl ether ([^{3}H]COE)-HDL was prepared as described previously [5]. In the third experiment, after 4 weeks of vehicle or CL316,243 treatment, mice were injected via the tail vein with [^{3}H]COE-labeled HDL (200,000 dpm per mouse). Blood was taken from the tail vein at 5 min, 1 h, 2 h, 4 h, 8 h, and 24 h after injection to determine the plasma decay of [^{3}H]COE-labeled HDL. After 24 h, mice were killed and transcardially perfused with ice-cold saline. Livers were isolated and weighed, and ^{3}H-activity was quantified.

***In vivo* plasma decay and hepatic uptake of VLDL-mimicking particles**

VLDL-mimicking particles (80 nm) were prepared as described previously [4], and labeled with both [^{3}H]dipalmitoylphosphatidylcholine (DPPC; PerkinElmer, USA) and [^{14}C] cholesteryl oleate ([^{14}C]CO). In the first experiment, after 9 weeks of vehicle or CL316,243 treatment, mice were fasted for 4 h and intravenously injected (t=0) with 200 μL of VLDL-mimicking particles (1 mg TG per mouse). Blood was taken from the tail vein at 2, 5, 10 and 15 min after injection to determine the plasma decay of [^{3}H]DPPC and [^{14}C]CO. To measure the time-dependent transfer of [^{3}H]DPPC onto HDL, ApoB-containing lipoproteins in the collected plasma samples were precipitated as described above. ^{3}H-activity was quantified in the supernatant. After 15 min, mice were killed and perfused with ice-cold saline. Liver was isolated and weighted, and ^{14}C-activity was quantified.

Gene expression analysis

In the first experiment, RNA was extracted from snap-frozen livers using Tripure RNA isolation reagent (Roche Diagnostics) according to the manufacturer's protocol. Total RNA (1 μg) was reverse transcribed using Moloney Murine Leukemia Virus (M-MLV) Reverse Transcriptase (Promega) for RT-qPCR according to the manufacturer's instructions to produce cDNA. mRNA expression was normalized to β-actin and *Gapdh* expression and expressed as fold change compared to vehicle-treated control mice using the ΔΔCT method. The primer sequences used are listed in **Supplemental Table I**.

Protein expression analysis

Snap-frozen organ samples obtained from the first experiment were lysed in 200-400 μL RIPA buffer containing 150 mM NaCl, 1.0% NP-40, 0.5% sodium deoxycholate, 0.1% sodium dodecyl sulphate and phosphatase inhibitor cocktail (Piece Thermo Fisher Scientific, IL, USA). Samples were homogenized with glass beads at 6.5 m·sec^{-1} with Advanced Bench-Top Bead Beating Lysis System (MP biomedicals, CA, USA) for 20 sec and then centrifugated at 16,200g for 15 min at 4°C to remove debris. Protein levels in the supernatant were determined using a bicinchoninic acid protein assay (Piece Thermo Scientific, IL, USA). Liver samples were diluted with sample buffer (Wes, ProteinSimple, CA, USA) to reach a protein concentration of 0.2 mg/mL and samples from gonadal white adipose tissue (gWAT), adrenals and aortas were diluted to 1.5 mg/L for subsequent Western blotting. A control sample was loaded to correct for potential variance between plates. Western blots were performed with capillary electrophoresis immunoassay using 12-230 kDa capillary cartridges (Wes, ProteinSimple, CA, USA) according to the manufacturer's protocol (https://www.proteinsimple.com/ebooks.html). The relative levels of each protein were automatically quantified (Wes, ProteinSimple, CA, USA). Results were normalized to the protein levels of GAPDH and expressed as fold change compared to means of the control group. Details of the

antibodies used are described in **the Major Resources Table**.

Atherosclerosis plaque characterization and quantification

After mice within the first experiment were killed as described above, hearts were collected, fixed in phosphate-buffered 4% formaldehyde, and embedded in paraffin. Four sections with 5 µm thickness of the aortic root area with 50 µm-intervals were used and stained with haematoxylin-phloxine-saffron for histological analysis. Lesions were categorized for lesion severity according to the guidelines of the American Heart Association adapted for mice and classified as mild lesions (types 1 - 3) or severe lesions (types 4 - 5) [6]. Monoclonal mouse antibody M0851 (1:1000; Dako, Heverlee, The Netherlands) against smooth muscle cell (SMC) actin was used to quantify the SMC area. Sections were stained with Sirius Red to quantify the collagen area. Macrophage area was determined using rat anti-mouse antibody MAC3 (1:1000; 0.5 µg/mL, BD Pharmingen, San Diego, CA, USA). Mouse IgG (1:1000, 50 ng/mL, BD Pharmingen, San Diego, CA, USA) and rat IgG (1:1000, 2 µg/mL; R&D systems) were used as negative controls. Lesion area and composition were determined with Image J Software (version 1.50i). The cellular and extracellular components were further compared as the ratio of SMC and collagen area to macrophage area. Please see **the Major Resources Table**.

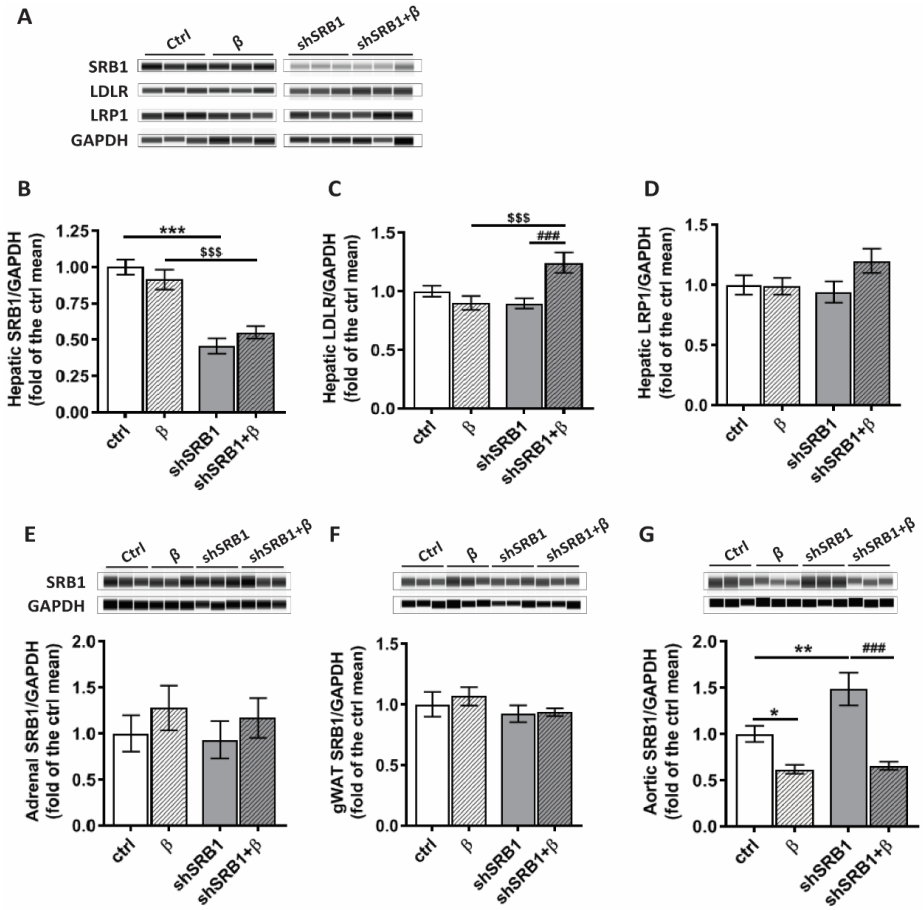

Supplemental Figure I. shSRB1-AAV8 selectively knocks down SRB1 protein in liver. *E3L.CETP* mice fed a WTD and pretreated with vehicle (ctrl) or an adeno-associated virus serotype 8 loaded with an shRNA targeting SRB1 (shSRB1) at week -2, were treated with vehicle or the β3-AR agonist CL316,243 (β) from week 0. At week 9, mice were killed and tissues were isolated to measure (**A, B**) SRB1, (**A**, **C**) LDL receptor (LDLR), (**A, D**) LDLR-related protein1 (LRP1) protein levels in the liver, and SRB1 protein levels in (**E**) adrenal glands, (**F**) gonadal white adipose tissue (gWAT), and (**G**) aorta (n = 10/11 mice per group). Three representative blots per group are showed. Values are means ± SEM. Differences between two groups were determined using two-way ANOVA followed by a Fisher's LSD post hoc test. *P<0.05, **P<0.01, ***P<0.001 vs. ctrl; $^{\$\$\$}$P<0.001 vs. β, $^{\#\#\#}$P<0.001 vs. shSRB1.

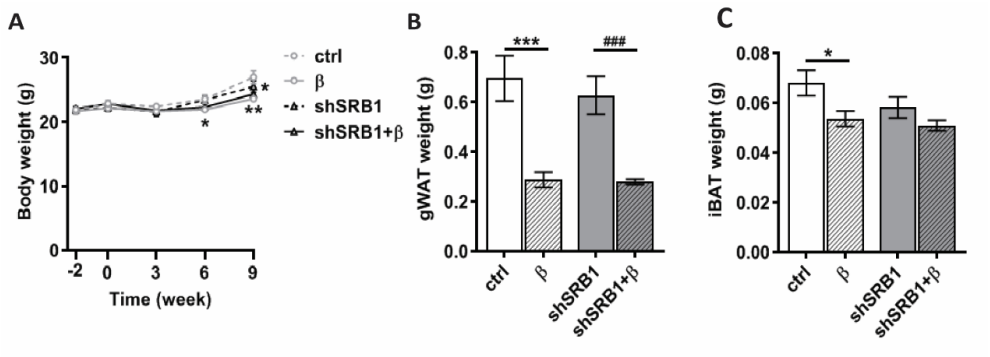

Supplemental Figure II. β3-AR agonism, but not hepatic SRB1 knockdown, reduces total body weight and gonadal white adipose weight**.** *E3L.CETP* mice fed a WTD and pretreated with vehicle (ctrl) or an adeno-associated virus serotype 8 loaded with an shRNA targeting SRB1 (shSRB1) at week -2, were treated with vehicle or the β3-AR agonist CL316,243 (β) from week 0. (**A**) Mice were weighed at the indicated time points. At week 9, mice were killed and (**B**) gonadal white adipose (gWAT), and (**C**) intrascapular brown fat (iBAT) were weighed (n= 10/11 mice per group) Values are means ± SEM. Differences between two groups were determined using two-way ANOVA followed by a Fisher's LSD post hoc test. *P<0.05, **P<0.01, ***P<0.001 vs. ctrl; $^{###}$P<0.001 vs. shSRB1.

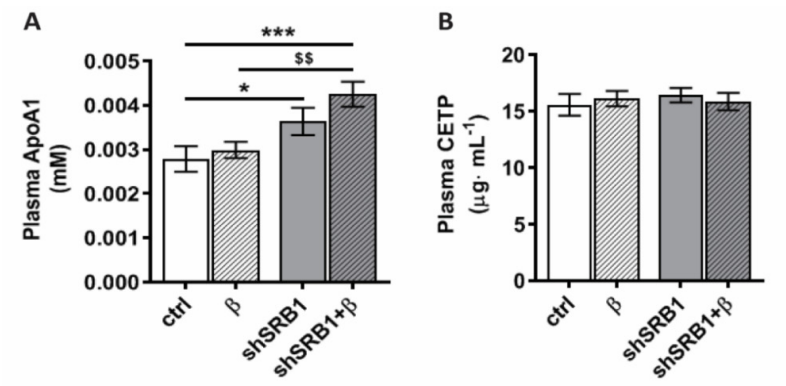

Supplemental Figure III. Hepatic SRB1 knockdown on top of β3-AR agonism increases **plasma ApoA1 levels without changing CETP levels.** *E3L.CETP* mice fed a WTD and pretreated with vehicle (ctrl) or an adeno-associated virus serotype 8 loaded with an shRNA targeting SRB1 (shSRB1) at week -2, were treated with vehicle or the β3-AR agonist CL316,243 (β) from week 0. At week 9, blood samples were collected to measure plasma levels of (**A**) ApoA1 and (**B**) CETP. (n= 10/11 mice per group) Values are means ± SEM. Differences between two groups were determined using two-way ANOVA followed by a Fisher's LSD post hoc test. *P<0.05, **P<0.01, ***P<0.001 vs. ctrl; $^{$$}$P<0.01 vs. β.

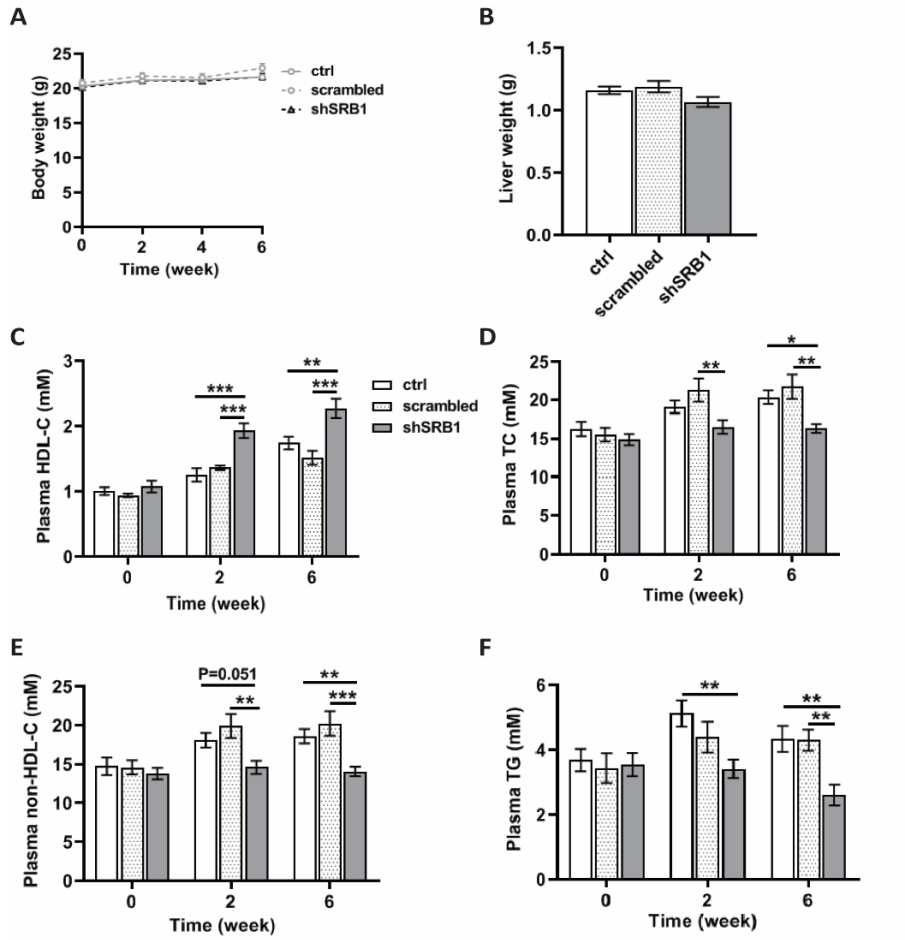

Supplemental Figure IV. AAV8 vector has no specific effects on body weight, liver weight and plasma lipid levels. *E3L.CETP* mice fed a WTD were treated with vehicle (ctrl), an adeno-associated virus serotype 8 loaded with a scrambled sequence (scrambled) or an shRNA targeting SRB1 (shSRB1) for 6 weeks. (**A**) Total body weight and (**B**) liver weight were measured during and after 6 weeks of treatment. Plasma (**C**) HDL-C, (**D**) total cholesterol (TC), (**E**) non-HDL-C, and (**F**) triglyceride (TG) levels were measured at indicated time points. (n= 9/10 mice per group) Values are means ± SEM. Difference between two groups was determined using one-way analysis of variance (ANOVA) with the *LSD post hoc* test. *P<0.05, **P<0.01, ***P<0.001 vs. shSRB1.

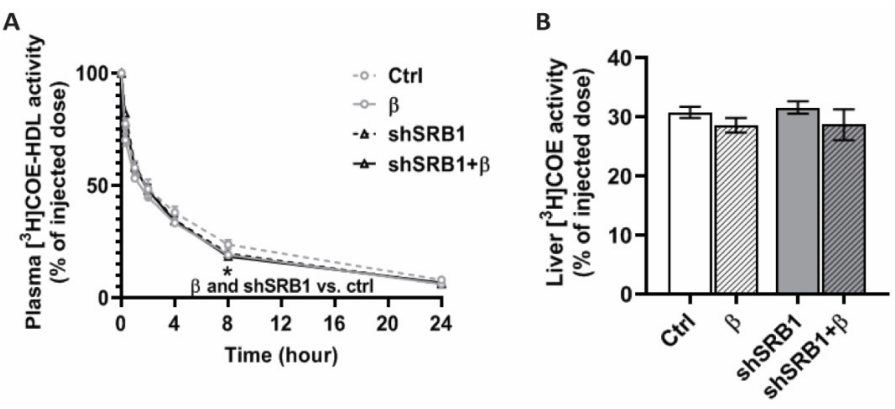

Supplemental Figure V. Hepatic SRB1 knockdown and β3-AR agonism do not influence HDL-cholesteryl oleyl ether kinetics. *E3L.CETP* mice fed a WTD and pretreated with vehicle (ctrl) or an adeno-associated virus serotype 8 loaded with an shRNA targeting SRB1 (shSRB1) at week -2, were treated with vehicle or the β3-AR agonist CL316,243 (β) from week 0. At week 4, mice were intravenously injected with [^{3}H]cholesteryl oleyl ether ([^{3}H]COE) labelled HDL. Plasma samples were collected at indicated time points, (**A**) plasma clearance of [^{3}H] COE-HDL was determined, and (**B**) hepatic uptake of [^{3}H]COE-HDL was measured after 24 h of injection. (n= 8-10 mice per group) Values are means ± SEM. Differences between two groups were determined using two-way ANOVA followed by a Fisher's LSD post hoc test. *P<0.05 vs. ctrl.

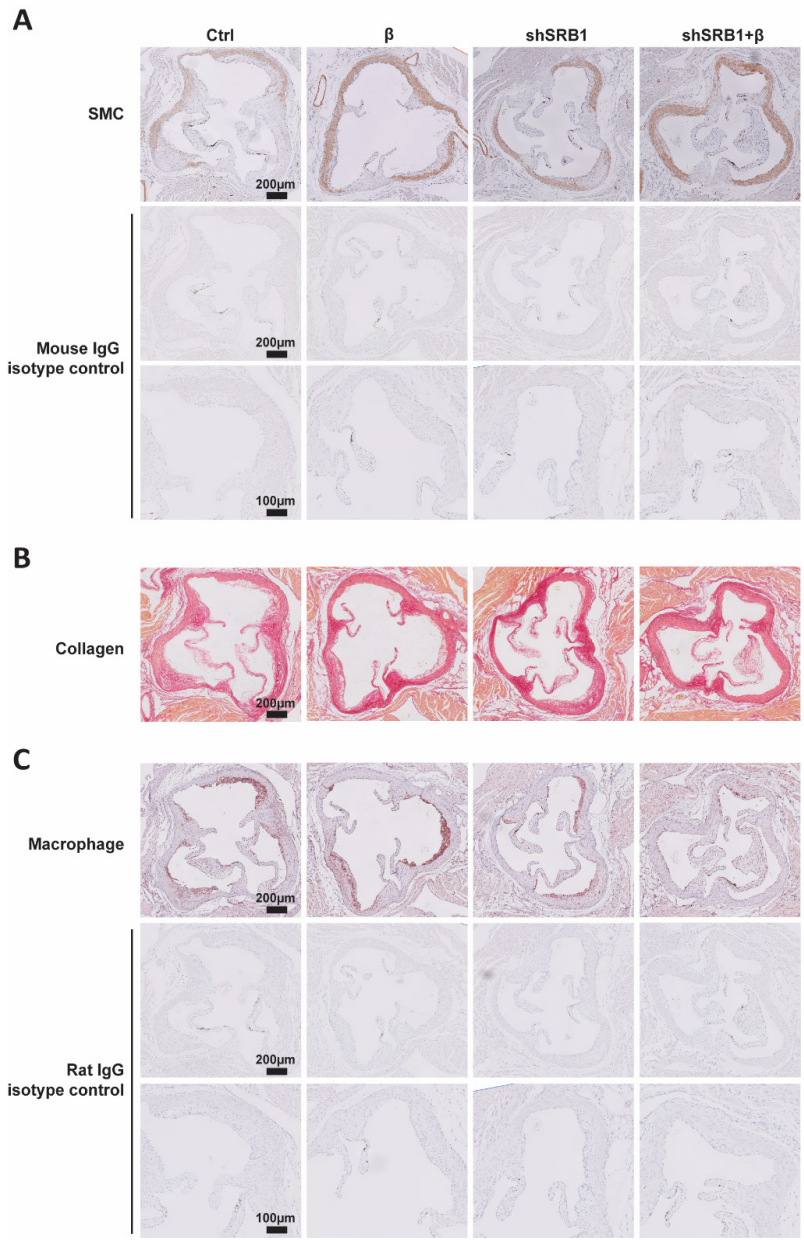

Supplemental Figure VI. Hepatic SRB1 knockdown on top of β3-AR agonism increases the ratio of smooth muscle cell and collagen area to macrophage area. *E3L.CETP* mice fed a WTD and pretreated with vehicle (ctrl) or an adeno-associated virus serotype 8 loaded with an shRNA targeting SRB1 (shSRB1) at week -2, were treated with vehicle or the β3-AR agonist CL316,243 (β) from week 0 for 9 weeks. Cross-sections of aortic root were stained for (**A**) smooth muscle cells (SMC), (**B**) collagen and (**C**) macrophages. Mouse IgG and rat IgG isotype antibodies were used as negative control staining of SMC and macrophages, respectively.

Supplemental Table I. Primer list

Gene	Forward	Reverse
Abca1	CCCAGAGCAAAAAGCGACTC	GGTCATCATCACTTTGGTCCTTG
Abcg1	AGGTCTCAGCCTTCTA-AAGTTCCTC	TCTCTCGAAGTGAAT-GAAATTTATCG
Angptl4	GGAAAGAGGCTTCCCAAGAT	TCCCAGGACTGGTTGAAGTC
Apoa1	GGAGCTGCAAGGGAGACTGT	TGCGCAGAGAGTCTACGTGTGT
Apob	GCCCATTGTGGACAAGTTGATC	CCAGGACTTGGAGGTCTTGGA
Apoc2	ACATTCAGGTCCCAGACAGC	AGGTCTTTGGCAACCTCCTT
CETP	CAGATCAGCCACTTGTCCAT	CAGCTGTGTGTTGATCTGGA
Gapdh	GGGGCTGGCATTGCTCTCAA	TTGCTCAGTGTCCTTGCTGGGG
Hl	CAGCCTGGGAGCGCAC	CAATCTTGTTCTTCCCGTCCA
Lcat	GGCAAGACCGAATCTGTTGAG	ACCAGATTCTGCACCAGTGTGT
Ldlr	GCATCAGCTTGGACAAGGTGT	GGGAACAGCCACCATTGTTG
Lpl	CCCTAAGGACCCCTGAAGAC	GGCCCGATACAACCAGTCTA
Lrp1	CAATGGGCTAAGCCTGGATA	CGGTACTCGGTCCAAAAGAG
Mttp	CTCTTGGCAGTGCTTTTTCTCT	GAGCTTGTATAGCCGCTCATT
Pcsk9	TGTGAGGTCCCACTCTGTG	GCTTCTGCTCCAGAGGTCA
Srb1	GTGCTGCTGGGGCTTGGAGG	CACTGGTGGGCTGTCCGCTG
Srebp1c	AGCCGTGGTGAGAAGCGCAC	ACACCAGGTCCTTCAGTGATTTGCT
β-actin	AACCGTGAAAAGATGAC-CCAGAT	CACAGCCTGGATGGCTACGTA

Abca1, ATP-binding cassette sub-family A member 1; Abcg1, ATP-binding cassette sub-family G member1; Angptl4, angiopoietin-like 4; Apoa1,apolipoprotein a1; Apob, apolipoprotein b; Apoc2, apolipoprotein c 2; CETP, cholesteryl ester transfer protein; Gapdh, glyceraldehyde-3-phosphate dehydrogenase; Hl, hepatic lipase; Lcat, lecithin : cholesterol acyltransferase; Ldlr, low density lipoprotein receptor; Lpl, lipoprotein lipase; Lrp1, low-density lipoprotein receptor related protein 1; *Mttp, microsomal triglyceride transfer protein; Pcsk9, proprotein convertase subtilisin-like kexin type 9. Srb1, scavenger receptor class type 1; Srebp1c, sterol regulatory element-binding protein 1c*

Supplemental Table II. Major Resources Table

Animals (in vivo studies)

Species	Vendor or Source	Background Strain	Sex
*APOE*3-Leiden* (*E3L*). CETP mice	Leiden University Medical Center	C57BL/6J	Female

Animal breeding

	Species	Vendor or Source	Background Strain
Parent – Male/Female	*APOE*3-Leiden* (*E3L*) mice	Leiden University Medical Center	C57BL/6J
Parent – Male/Female	CETP transgenic mice	Leiden University Medical Center	C57BL/6J

Antibodies

Target antigen	Vendor or Source	Catalog #	Working concentration
MAC3	Rat	BD Pharmingen, 553322	1:1000 (0.5 µg/mL)
Smooth muscle actin	Mouse	Dako M0851	1:1000 (working solution is unknown)
SRB1	Rabbit	ab52629, Abcam	1:100 (2 µg/mL)
LRP1	Rabbit	ab92544, Abcam	1:500 (0.4 µg/mL)
LDLR	Goat	AF2255, R&D system	1:50 (4 µg/mL)
GAPDH	Rabbit	5174S, Cell Signaling Technology	1:40 (0.85 µg/mL)
Anti-rabbit secondary antibody	Not applicable	DM-001, Proteinsimple	Ready to use (10 µL per well for Western blotting)
Anti-goat secondary antibody	Not applicable	DM-006, Proteinsimple	Ready to use (10 µL per well for Western blotting)

Supplemental references

1. Daugherty, A., et al., *Recommendation on Design, Execution, and Reporting of Animal Atherosclerosis Studies: A Scientific Statement From the American Heart Association.* Arterioscler Thromb Vasc Biol, 2017. **37**(9): p. e131-e157.
2. van Eyk, H.J., et al., *Hepatic triglyceride content does not affect circulating CETP: lessons from a liraglutide intervention trial and a population-based cohort.* Sci Rep, 2019. **9**(1): p. 9996.
3. Zechner, R., *Rapid and simple isolation procedure for lipoprotein lipase from human milk.* Biochim Biophys Acta, 1990. **1044**(1): p. 20-5.
4. Rensen, P.C., et al., *Selective liver targeting of antivirals by recombinant chylomicrons--a new therapeutic approach to hepatitis B.* Nat Med, 1995. **1**(3): p. 221-5.
5. van der Hoogt, C.C., et al., *Fenofibrate increases HDL-cholesterol by reducing cholesteryl ester transfer protein expression.* J Lipid Res, 2007. **48**(8): p. 1763-71.
6. Wong, M.C., et al., *Hepatocyte-specific IKKbeta expression aggravates atherosclerosis development in APOE*3-Leiden mice.* Atherosclerosis, 2012. **220**(2): p. 362-8.